

Research on an Assembly Method for Large Irregular Thin-Walled Components Based on a Six-Axis Industrial Robot

Haoran Liu *

School of Mechanical Engineering, Tianjin University of Technology and Education, Tianjin 300222, China

* Corresponding Author: Haoran Liu

ABSTRACT

To address the challenges of low stiffness, high deformability, weak positioning references, and the coexistence of multiple constraint bases during the assembly of large and complex thin-walled components, an automated assembly method based on a six-axis industrial robot integrated with binocular vision is proposed, enabling high-precision and coordinated docking in the assembly process of large irregular thin-walled parts. First, an error propagation analysis is conducted for the irregular thin-walled components, and the maximum allowable deviation domain in both translational and rotational spaces that ensures successful assembly is derived. On this basis, a staged assembly strategy following the principle of “initial positioning, primary docking, and secondary constraint” is proposed. The robot first uses binocular vision to estimate the pose deviation of thin-walled part 1 with respect to the locating pins on the fixed base and plans the target TCP pose to achieve pin-hole alignment. Subsequently, the tongue-and-groove (rabbet) mating between thin-walled parts 1 and 2 is performed. Finally, thin-walled part 2 is guided by vision to align with the locating pins on the movable base, completing secondary positioning and constraint, thereby realizing a multi-datum closed-loop assembly. An adaptive pose-error compensation mechanism is incorporated into the assembly process, enabling the robot to satisfy geometric assembly constraints even in the presence of initial fixturing errors and elastic deformations of the thin-walled components. The experimental results demonstrate that, under the combined constraints of binocular reconstruction errors and the robot’s repeatability, the proposed method can reliably achieve multi-datum automatic assembly of large-scale irregular thin-walled components. It significantly reduces the reliance on manual alignment and improves both the assembly success rate and consistency, providing an effective technical pathway for the robotic assembly of large flexible structures.

KEYWORDS

Large Irregular Thin-walled Components; Pose Estimation; Assembly Deviation Modeling; Flexible Structure Assembly.

1. INTRODUCTION

With the increasing demand for lightweight structures and functional integration in aerospace, rail transit, and large-scale equipment manufacturing, large irregular thin-walled components are widely used in aircraft skins, fuselage frames, and high-end structural assemblies due to their low mass, low stiffness, and complex geometries. However, such components commonly suffer from large deformations, unstable assembly datums, and coupled multi-constraint conditions during assembly, making conventional methods that rely on manual experience or rigid fixtures incapable of simultaneously ensuring efficiency and accuracy, thereby becoming a critical bottleneck for advanced manufacturing automation.

In recent years, with the rapid development of robotics[1], sensing technologies[2], and image recognition techniques[3], automated assembly methods integrating industrial robots with machine vision have provided a new technological pathway for the intelligent assembly of complex components. Industrial robots offer high motion flexibility and excellent repeatability, enabling them to perform grasping, positioning, and assembly tasks within large workspaces, while binocular vision-based three-dimensional perception can acquire the spatial pose and key geometric features of workpieces in real time, thereby providing online positioning and error compensation capabilities for robotic systems. Yizhen Zheng[4] proposed a vision-guided manual assembly method for blind-area operations by integrating augmented reality with path planning and pose estimation to address blind-spot assembly problems. A hybrid Rapidly Exploring Random Tree*-Artificial Potential Field (RRT*-APF) algorithm was developed to search for feasible collision-free arm trajectories within the assembly workspace, and the results demonstrated that the proposed method can significantly improve the efficiency of blind-area assembly while effectively reducing assembly errors. Chenyu Liu[5] addressed the on-site assembly of prefabricated components by proposing a vision-based robot-assisted installation system, in which a crane is used for coarse alignment and two robots cooperate to finely adjust the position and orientation of the components, thereby completing the assembly of prefabricated structures

Existing studies have shown that vision-guided assembly has achieved favorable performance in the grasping and docking of rigid parts; however, significant challenges remain for the assembly of large-scale, low-stiffness, and multi-constrained thin-walled components. Rui Guo[6] addressed the docking difficulties caused by large and irregular parts by proposing a method that estimates the relative pose of mating components based on feature-point coordinate fitting, and achieved precise docking of large components through industrial robot control. Zechen Li[7] proposed a pose-deviation measurement and adjustment method for flexible docking of spacecraft modules based on the common perpendicular and the spatial center of the docking contact surfaces. The docking process was divided into axis-parallel alignment and axis-coincident alignment stages, and a composite sinusoidal function was adopted for joint-space trajectory planning, enabling integrated measurement and adjustment of docking pose deviations. Zhou Y[8] proposed a novel autonomous charging and docking method for intelligent unmanned vehicles based on infrared guidance and vision-assisted positioning.

To address the assembly problem of large irregular thin-walled components, this paper proposes an automated assembly method based on binocular vision and a six-axis industrial robot. By visually recognizing key features of the thin-walled components and estimating their poses, a geometric constraint model is established to derive the maximum allowable pose deviation that ensures successful assembly, based on which a staged, multi-constraint vision-guided assembly process is designed. The proposed method aims to achieve stable and high-precision automated assembly of large irregular thin-walled components in the presence of manufacturing errors, fixturing errors, and elastic deformations.

2. OVERALL DESIGN OF THE AUTOMATED ASSEMBLY SYSTEM

To achieve high-precision automated assembly of large irregular thin-walled components under multi-datum conditions, a docking system composed of a six-axis industrial robot, a binocular vision system, and dedicated docking fixtures is developed in this study. The assembly objects consist of two large irregular thin-walled parts, referred to as thin-walled part 1 and thin-walled part 2. The overall assembly system mainly comprises three subsystems—the docking fixtures, the industrial robot, and the binocular vision system—as illustrated in Figure 1.

As shown in Figure 2, the docking platform consists of a fixed base, a movable base, and a supporting fixture located between them. The fixed base provides the primary positioning datum for thin-walled part 1 and is equipped with two locating pins that form pin-hole constraints with the two

corresponding holes on one side of thin-walled part 1. The movable base serves as a secondary positioning datum for thin-walled part 2 and is also equipped with two locating pins that mate with the pin holes on one side of thin-walled part 2. A supporting fixture is arranged between the two bases to provide gravitational support and shape retention for the thin-walled components during assembly, thereby preventing excessive elastic deformation induced by their own weight.

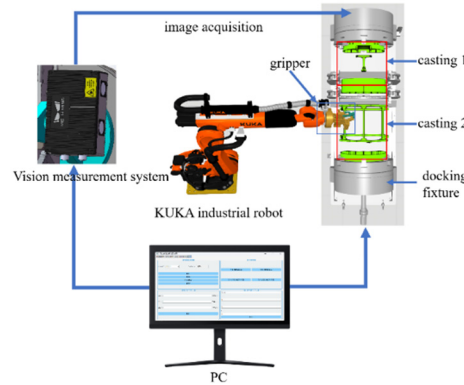


Figure 1. Hardware composition of the docking system

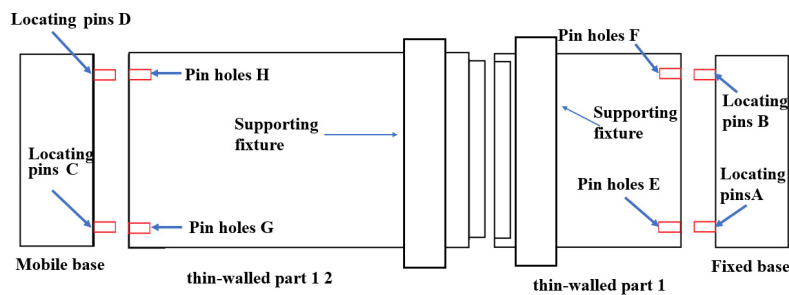


Figure 2. schematic of thin-walled segment docking

The six-axis industrial robot is installed on one side of the docking platform and uses its end effector to grasp the thin-walled components for handling and docking operations. Owing to its large workspace and high repeatability, the robot is able to cover all assembly trajectories between the fixed base, the movable base, and the storage area of the thin-walled parts. The binocular cameras are employed to acquire three-dimensional feature information of both the thin-walled components and the locating pins on the bases, providing the necessary data for assembly pose estimation.

3. DEVIATION MODELING AND ASSEMBLY METHOD DESIGN

3.1. Assembly Deviation Modeling of Thin-Walled Components

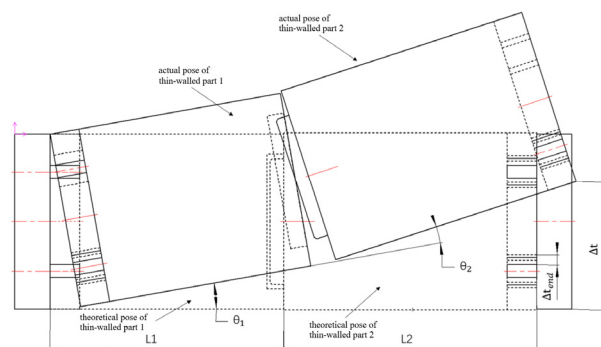


Figure 3. overall deviation model of the segment assembly

During vision-guided robotic assembly of thin-walled components, their spatial poses are inevitably affected by binocular reconstruction errors, robot grasping errors, manufacturing tolerances, and elastic deformations of the components themselves, resulting in systematic deviations between the actual and ideal assembly poses. To characterize the influence of these deviations on the feasibility of pin-hole and tongue-and-groove (rabbet) assemblies, a unified pose error model is established, and the overall variation model of assembly deviations is illustrated in Figure 3.

Let the pose of the thin-walled component relative to the assembly datum in the ideal assembly state be given by Equation 1.

$$T_0 = \begin{bmatrix} R_0 & p_0 \\ 0 & 1 \end{bmatrix} \quad (1)$$

Here, R_0 and p_0 denote the ideal orientation and position, respectively. The pose of the thin-walled component in the actual assembly process can be expressed by Equation 2.

$$T = T_0 \Delta T \quad (2)$$

In Equation 2, ΔT represents the pose perturbation induced by various error sources. Under small-deviation conditions, it can be linearized as Equation 3.

$$\Delta T \approx \begin{bmatrix} I + [\theta]_{\times} & \delta \\ 0 & 1 \end{bmatrix} \quad (3)$$

where $\delta = [\delta_x, \delta_y, \delta_z]^T$ denotes the translational error of the thin-walled component, $\theta = [\theta_x, \theta_y, \theta_z]^T$ represents the small rotational errors about the three axes, and $[\cdot]_{\times}$ is the skew-symmetric matrix operator.

For the pin-hole assembly, let the center of the i -th hole on the thin-walled component be located at r_i with respect to the component coordinate frame in the ideal state. When a pose error exists, the actual offset of this hole center in the base coordinate frame can be expressed by Equation 4.

$$\Delta e_i = \delta + \theta \times r_i \quad (4)$$

This offset contains both the translational error and the position error amplified by the rotational deviation. Let r_p and r_h denote the radii of the pin and the hole, respectively, and the radial assembly clearance be $c = r_h - r_p$; then the necessary condition for successful pin-hole insertion is given by Equation 5.

$$\|\Delta e_i\| \leq c, i = 1, 2 \quad (5)$$

That is, the spatial offsets of both holes must lie within their respective assembly clearance ranges. It follows that the orientation error of a thin-walled component is significantly amplified with increasing distance from the pin-hole to the reference origin, making large-scale thin-walled components particularly sensitive to such errors.

For the tongue-and-groove (rabbet) mating between thin-walled part 1 and thin-walled part 2, the assembly constraints can be equivalently expressed as limitations on the relative translational and rotational errors in a six-dimensional pose space. Let the relative pose error of thin-walled part 2 with respect to thin-walled part 1 be $(\delta_{21}, \theta_{21})$; the rabbet structure requires that the displacements in the tangential and normal directions, as well as the rotations about each axis, do not exceed the limits permitted by the geometric clearances of the rabbet, which collectively define the feasible assembly domain.

Since thin-walled part 2 must ultimately form a secondary mating with the locating pins on the movable base in this system, its overall error relative to the movable base results from the superposition of the residual error of thin-walled part 1 with respect to the fixed base and the residual error of thin-walled part 2 with respect to thin-walled part 1, which can be expressed by Equation 6.

$$\Delta T_{2M} = \Delta T_{21} \Delta T_{1F} \quad (6)$$

This error propagation relationship indicates that multi-datum assembly is not merely a local docking problem, but rather a cascaded system in which errors are progressively amplified. Therefore, pose deviations must be actively constrained and controlled at each assembly stage; otherwise, even if individual docking steps satisfy tolerance requirements, the final pin-hole mating may still fail.

3.2. Assembly Method Design

Based on the aforementioned pose deviation model, the assembly of large irregular thin-walled components is essentially a process of progressively compressing and regulating six-dimensional pose errors under multiple constraints. If a simple strategy of “vision measurement–single alignment–direct insertion” is adopted, errors are prone to be amplified within the cascaded pin-hole and rabbet–rabbet structures, leading to assembly failure. Therefore, the assembly process is designed as a staged vision-guided procedure with controllable deviations, ensuring that the residual error at each stage is constrained within the allowable assembly domain of the subsequent stage.

As shown in Figure 4, the robot first grasps thin-walled part 1, and during its assembly with the fixed base, the binocular vision system acquires the three-dimensional coordinates of the two pin holes on thin-walled part 1 and matches them with the calibrated coordinates of the two locating pins on the fixed base. The pose deviation of thin-walled part 1 relative to the ideal assembly pose, denoted as $(\delta_{1F}, \theta_{1F})$, can thus be obtained. According to the pin-hole deviation model, the target TCP pose of the robot is not set to make the hole centers exactly coincide with the pin centers; instead, it is planned such that the offsets of both holes fall within the central region of the assembly clearance circles. This strategy satisfies the insertion conditions while maximizing the residual error margin, effectively preventing edge interference caused by slight orientation deviations during contact and preserving usable deviation space for the subsequent assembly of thin-walled part 2.

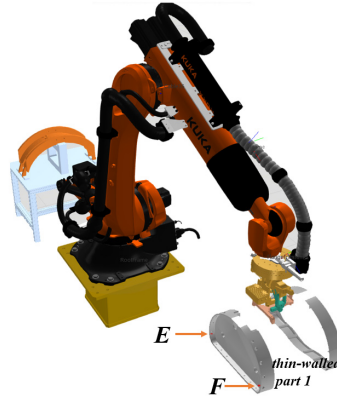


Figure 4. Robot grasping thin-walled part 1

After thin-walled part 1 is docked with the fixed base, its residual pose error is fixed and serves as the reference datum for the assembly of thin-walled part 2. The robot then grasps thin-walled part 2, as shown in Figure 5, and the binocular camera detects its rabbet features and performs spatial registration with the rabbet model of thin-walled part 1 to compute the pose error of thin-walled part 2 relative to thin-walled part 1, denoted as $(\delta_{21}, \theta_{21})$. According to the geometric constraints of the rabbet mating, the assembly objective is no longer merely to minimize translational errors, but rather to optimize the rotational error components so that the mating surfaces of the rabbets remain as coplanar and coaxial as possible, thereby reducing the hole-position deviations amplified by the lever-arm effect of orientation errors. This orientation-priority docking strategy can significantly attenuate the transmission of errors toward the movable base.

After thin-walled part 2 is mated with thin-walled part 1 through the rabbet joint, the overall spatial error of thin-walled part 2 is formed by the superposition of the two previous assembly residuals. At

this stage, the binocular vision system remeasures the pin holes on thin-walled part 2 and matches them with the coordinates of the locating pins on the movable base to obtain the current residual error (δ_{2M}, θ_{2M}). The robot then performs small-range vision-guided fine adjustments, driving the spatial offsets of both holes to converge within the pin-hole assembly clearance, thereby achieving stable insertion under the final secondary datum constraints.

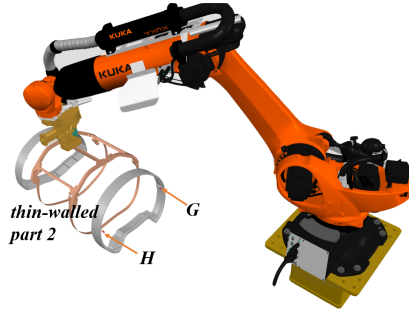


Figure 5. Robot grasping thin-walled part 2

Through a closed-loop framework of visual perception, error estimation, in-domain optimization, and staged docking, the proposed assembly method ensures that the pose errors of the thin-walled components are always confined within the feasible assembly domain in the multi-datum cascaded system. This effectively prevents uncontrolled error accumulation that could lead to assembly failure, thereby enabling reliable robotic assembly of large irregular thin-walled components under conditions of measurement errors and elastic deformations.

4. EXPERIMENTAL ANALYSIS

To verify the feasibility and effectiveness of the proposed binocular vision-based and six-axis industrial robot-assisted assembly method for large irregular thin-walled components under multi-datum constraints, a complete assembly system model was established in the KUKA. Sim Pro simulation environment, and the grasping, visual localization, and three-stage docking processes of the thin-walled components were simulated. The simulation model includes a six-axis KUKA industrial robot, an end effector, a fixed base, a movable base, a supporting fixture, and two large irregular thin-walled components.

In the simulation, translational and rotational perturbations were intentionally introduced into the initial poses of the thin-walled components to emulate the initial pose deviations caused by binocular vision measurement errors, grasping errors, and component deformations, thereby evaluating the robustness of the proposed assembly method under non-ideal conditions. The measured initial positions of the feature points are listed in Table 1.

Table 1. Initial positions of feature points

Feature points	X	Y	Z
A	1205.18	-865.40	1002.50
B	1765.18	-865.40	1002.51
C	1175.20	878.59	1002.50
D	1795.20	878.59	1002.51
E	21.44	1505.18	240.50
F	21.44	2065.18	240.50
G	-654.80	1315.40	305.50
H	-1274.80	1315.40	305.50

According to the proposed assembly method, the following assembly procedure was implemented in the simulation: the robot first grasps thin-walled part 1 from the storage location and moves it toward

the fixed base; the target TCP pose is then computed based on the pose data provided by the vision system, and the pin-hole docking between thin-walled part 1 and the fixed base is executed, as shown in Figure 6.

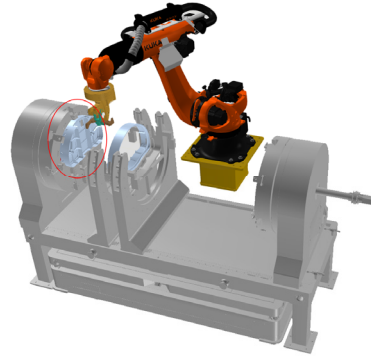


Figure 6. Thin-walled part 1 docked with the fixture

Subsequently, the robot grasps thin-walled part 2 and performs the rabbet mating under the condition that thin-walled part 1 has been positioned. After thin-walled part 2 is docked with thin-walled part 1, the robot is guided by visual feedback to complete the final pin-hole docking between thin-walled part 2 and the movable base, as shown in Figure 7. After assembly, the coordinates of the feature points are listed in Table 2.

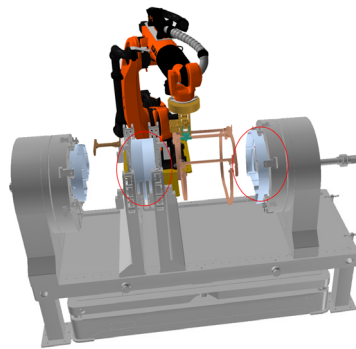


Figure 7. Assembly completed

Table 2. Feature point coordinates after docking

Feature points	X	Y	Z
A	1205.18	-865.40	1002.50
B	1765.18	-865.40	1002.51
C	1175.20	860.60	1002.50
D	1795.20	860.60	1002.51
E	1205.18	-865.41	1002.51
F	1765.18	-865.41	1002.51
G	1175.18	860.59	1002.50
H	1795.18	860.59	1002.50

After the assembly is completed, the theoretical and actual positions of the feature points are compared based on Tables 1 and 2, and the results are summarized in Table 3.

It can be observed that, even in the presence of initial pose errors, the proposed staged vision-guided assembly method enables thin-walled part 1 to be stably inserted into the locating pins of the fixed base, ensures a smooth rabbet mating process between thin-walled parts 1 and 2, and ultimately achieves reliable pin-hole engagement between thin-walled part 2 and the movable base. The simulation results demonstrate that, by uniformly modeling the pin-hole and rabbet-rabbet assembly constraints and adopting a staged, error-controlled assembly strategy, the accumulation and

amplification of errors in the multi-datum cascaded system can be effectively suppressed, allowing stable automated assembly of large irregular thin-walled components even in the presence of measurement errors and structural flexibility.

Table 3. Errors between theoretical and actual feature point positions after docking

Feature point	coordinates	Measured value	Theoretical value	Error
E	E_x	1205.18	1205.18	0.00
	E_y	-865.41	-865.40	-0.01
	E_z	1002.51	1002.50	0.01
F	F_x	1765.18	1765.18	0.00
	F_y	-865.41	-865.40	-0.01
	F_z	1002.51	1002.51	0.00
G	G_x	1175.18	1175.20	-0.02
	G_y	860.59	860.60	-0.01
	G_z	1002.50	1002.50	0.00
H	H_x	1795.18	1795.20	-0.02
	H_y	860.59	860.60	-0.01
	H_z	1002.50	1002.51	-0.01

5. SUMMARY

This study addresses the challenge of achieving high-precision automated assembly of large irregular thin-walled components under multi-datum constraints by proposing a vision-guided assembly method based on binocular vision and a six-axis industrial robot. A multi-constraint assembly system model composed of a fixed base, a movable base, a supporting fixture, and two thin-walled components is established, and the geometric constraints of the pin-hole and rabbet-rabbet mating pairs are explicitly defined. By developing a unified pose deviation model, the effects of vision measurement errors, grasping errors, and elastic deformations on assembly accuracy are analyzed, and the mechanisms of error propagation and amplification in the multi-datum cascaded structure are revealed. On this basis, a staged vision-guided assembly strategy with controlled deviations is designed to effectively suppress error accumulation along the assembly chain. The proposed method is validated in the KUKA. Sim Pro simulation environment, where stable docking between the thin-walled components and the bases, as well as between the components themselves, is achieved even in the presence of initial pose errors, demonstrating both the effectiveness and engineering feasibility of the approach. This work provides a viable technical pathway for high-precision robotic assembly of large flexible thin-walled structures.

CONFLICTS OF INTEREST

The authors declare that they have no conflict of interest.

REFERENCES

- [1] Kodaira N. Expected innovation in industrial robots[J]. *Advanced Robotics*, 2016, 30(17-18): 1088-1094. <https://doi.org/10.1080/01691864.2016.1197794>.
- [2] Fujishima M, Ohno K, Nishikawa S, et al. Study of sensing technologies for machine tools[J]. *CIRP Journal of Manufacturing Science and Technology*, 2016, 14: 71-75. <https://doi.org/10.1016/j.cirpj.2016.05.005>.
- [3] Sun M, Zhao H. A Metric Learning-based Image Recognition Method[J]. *International Journal on Artificial Intelligence Tools*, 2022, 31(04): 2240012. <https://doi.org/10.1142/s0218213022400127>.
- [4] Zheng Y, Li Y, Wu W, et al. Visual guidance method for artificial assembly in visual blind areas based on augmented reality [J]. *The International Journal of Advanced Manufacturing Technology*, 2024, 134(1): 969-985. <https://doi.org/10.1007/s00170-024-14181-8>.

- [5] Liu C, Wu J, Jiang X, et al. Automatic assembly of prefabricated components based on vision-guided robot[J]. *Automation in Construction*, 2024, 162: 105385. <https://doi.org/10.1016/j.autcon.2024.105385>.
- [6] Guo Rui, Du Jinsong, Zheng Dechao, Lu Bolin, Yin Jian. A study on large parts precision docking method based on 6-axis industrial robot[J]. *Journal of Physics: Conference Series*, 2019, <https://doi.org/10.1088/1742-6596/1303/1/012041>.
- [7] Li Zechen, Jin Xin, Hao Juan, Zhang Wei, Zheng Xinhao, Cao Tongtai, Xu Zhengyu. Research on the assembly method of missile based on laser scanning[A] 2021: <https://doi.org/10.1117/12.2603152>.
- [8] Zhou Yunya, He Yang, Yan Yu, Li Fang, Li Neng, Zhang Chaofeng, Lu Zijian, Yang Zhiyong. Autonomous charging docking control method for unmanned vehicles based on vision and infrared[J]. *Journal of Physics: Conference Series*, 2023, 2584 (1): <https://doi.org/10.1088/1742-6596/2584/1/012065>.